Experimental Investigation of Indirect Field Oriented Control of Field Programmable Gate Array Based Five-Phase Induction Motor Drive

G. Renuka Devi

***Abstract*—**This paper analyzes the experimental investigation of indirect field oriented control of Field Programmable Gate Array (FPGA) based five-phase induction motor drive. A detailed *d-q* modeling and Space Vector Pulse Width Modulation (SVPWM) technique of 5-phase drive is elaborated in this paper. In the proposed work, the prototype model of 1 hp 5-phase Voltage Source Inverter (VSI) fed drive is implemented in hardware. SVPWM pulses are generated in FPGA platform through Very High Speed Integrated Circuit Hardware Description Language (VHDL) coding. The experimental results are observed under different loading conditions and compared with simulation results to validate the simulation model.

***Keywords*—**Five-phase induction motor drive, field programmable gate array, indirect field oriented control, multi-phase, space vector pulse width modulation, voltage source inverter, very high speed integrated circuit hardware description language.

I. Introduction

RECENTLY, multiphase machines have made a great impact on research. Some of the advantages of these machines are lower torque pulsation, reduction in harmonic currents, reduced stator current per phase without increasing the phase voltage [1]-[7]. When it is compared to three phase machine, it has greater reliability, fault tolerant feature and increased power in the same frame. These features can justify the higher complexity of the multiphase drive in special custom applications, such as electrical ship propulsion, traction drives, electric/hybrid vehicles, high power pumps and aerospace [8]-[15]. In order to improve the dynamic performance of multi-phase induction motor drives (MPIM), various induction motor control techniques are used nowadays. Along with variable frequency AC inverters, the concept of vector control has opened up a new possibility that induction motors can be controlled to achieve dynamic performance as good as that of DC or brushless DC motors. The two high-performance control strategies for MPIM are field-oriented control (FOC) and direct torque control (DTC). The drawbacks of DTC are; difficult to control torque and flux at very low speed, high current and torque ripple, variable switching frequency behaviour, high noise level at low speed and lack of direct current control. The above said drawbacks are overcome by FOC scheme. An IFOC scheme for a five-phase machine is discussed in [16]-[21]. It is identical to the corresponding vector control scheme for a three-phase machine. Vector control with a higher torque density which can be achieved in a five-phase machine, is analyzed in [20]. Detailed investigations on a multi-phase inverter fed multi-phase FOC drive is discussed in [22]. It is seen that verifications of simulation are available for various even and odd supply phase numbers. The d–q axis model of the IFOC of MPIM is discussed in [23]. It is well-known that control techniques are quite complicated in on line implementations to decouple the interaction between flux control and torque control of an induction motor. Hence, the algorithm computation is time consuming and its implementation usually requires a high performance DSP chip. DSP implementation open-loop constant v/f control scheme of a five-phase induction motor drive is reported in [24]. The DSP processors are limited by fixed hardware architecture and the sequential execution of instruction is more time consuming. A typical 150 MHz DSP processor with 300 MMASC (Millions Multiply-accumulate operations per second) has an approximate loop response time of 25μs. Therefore, fast and economical software is needed to carry out the modulation task and the control processes for multi-phase drive. A FPGA is more appropriate platform for online and real-time implementation of closed loop algorithm. Today's FPGA high-speed performance with parallelism leads to a drastic reduction of the execution time. In a 20 MHz FPGA processor with 1160 MMASC has an approximate loop response time of 0.2 μs. The FPGA implementation of five-phase VSI with three different space vectors are elaborated and discussed in [25]. FPGA based IFOC of the five-phase induction motor is carried out in this paper.

In this paper, d1-q1 modeling of 5-phase induction motor is presented. The SVPWM technique with large space vector for the 5-phase VSI is discussed. An indirect FOC based closed loop controller is designed to track the desired speed at varying loads. Finally, a comparison between the simulation and experimental results are presented.

This paper is organized as follows. Section II deals with the system description of 5-phase drive. Section III presents the IFOC control of 5-phase induction motor. Section IV discusses the verification of simulation results. Section V and Section VI describe the experimental setup and experimental results. Section VII concludes this paper.

Dr. G. Renuka Devi, Associate Professor, is with the Department of Electrical and Electronics Engineering, Manakula Vinayagar Institute of Technology, Puducherry, India (e-mail: renukadeviayyappan@gmail.com).

II. System Description of 5-Phase Drive

A. Power Circuit of Five-Phase VSI

The power circuit of VSI and phase displacement of five-phase is shown in Figs. 1 (a) and (b). The five-phase VSI is connected with five-phase induction motor load. The phases are mutually displaced by $2\pi/5$ rad. The input dc supply is obtained from a single-phase or 3-phase utility power supply through a diode bridge rectifier circuit. The voltages V_a, V_b, V_c, V_d, and V_e, are the inverter pole voltages connected to load terminals. The switching states of each pole should be combined with each other pole to create the required 5-phase output voltages. The phase voltages of the inverter and modulation index are given in (1) and (2). The Modulation Index (MI) is the control parameter of the inverter which adjusts the output voltage of the inverter according to the amplitude of the reference waveform. It is defined as the ratio of magnitude of the reference to magnitude of the carrier signals. The five-phase VSI has two pairs of line-to-line voltages (adjacent side *a* and *b*/ non-adjacent side *a* and *c*). The maximum value of the line-to-line voltage of 1.902 V is achieved in the non-adjacent side.

$$\begin{aligned}
V_{aN} &= \frac{n-1}{n}V_a - \frac{1}{n}(V_b + V_c + V_d + V_e)\\
V_{bN} &= \frac{n-1}{n}V_b - \frac{1}{n}(V_a + V_c + V_d + V_e)\\
V_{cN} &= \frac{n-1}{n}V_c - \frac{1}{n}(V_a + V_b + V_d + V_e)\\
V_{dN} &= \frac{n-1}{n}V_d - \frac{1}{n}(V_a + V_b + V_c + V_e)\\
V_{eN} &= \frac{n-1}{n}V_e - \frac{1}{n}(V_a + V_b + V_c + V_d)
\end{aligned} \tag{1}$$

$$MI = \frac{V_{ref}}{V_{tri}} \tag{2}$$

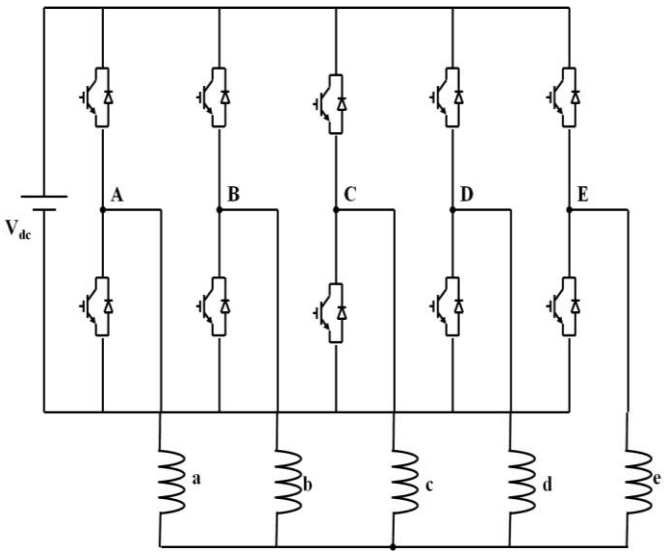

(a)

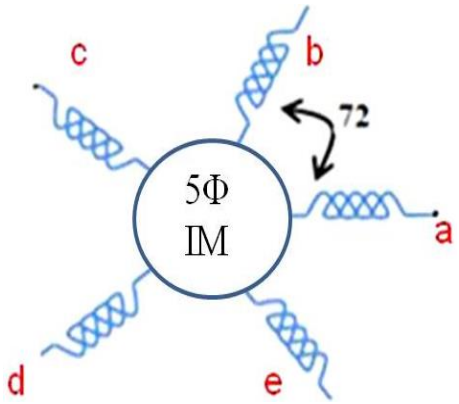

(b)

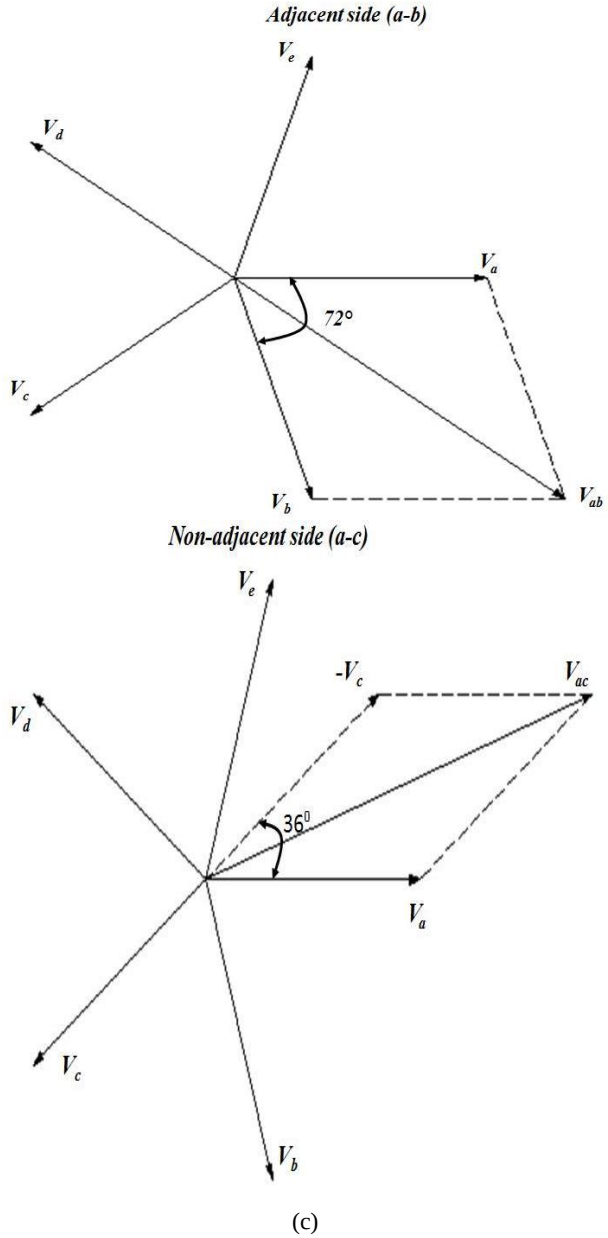

(c)

Fig. 1 (a) Power circuit of five-phase VSI (b) Phase displacement (c) Adjacent and Non-adjacent phase displacement of 5-phase system

The line and phase voltage of the 5-phase is derived from

(3)-(5). The maximum line to line voltage is attained in the non-adjacent side.

$$\begin{aligned} V_a &= V_m \angle 0° \\ V_b &= V_m \angle -72° \\ V_c &= V_m \angle -144° \\ V_d &= V_m \angle -216° \\ V_e &= V_m \angle -288° \end{aligned} \tag{3}$$

where $V_a=V_b=V_c=V_d=V_e=V_{ph}=V_m$ and $V_{ab}=V_{ac}=V_l$

The adjacent line voltage (V_{ab}) is

$$\begin{aligned} V_{ab} &= V_a - V_b = V_m \angle 0° - V_m \angle -72° \\ &= V_m[(Cos0° - jSin0°) - (Cos72° - jSin72°) \\ &= V_m[1 - 0.309 - j0.9510] \\ &= V_m[0.691 - j0.6510] \end{aligned} \tag{4}$$

Converting to polar form,

$$V_{ab} = 1.1755 V_m \angle 36°$$

The non-adjacent line voltage (V_{ac}) is

$$\begin{aligned} V_{ac} &= V_a - V_c = V_m \angle 0° - V_m \angle -144° \\ &= V_m[(Cos0° - jSin0°) - (Cos144° - jSin144°) \\ &= V_m[1 + 0.809 - j0.5877] \\ &= V_m[1.809 - j0.5877] \end{aligned} \tag{5}$$

Converting to polar form,

$$V_{ac} = 1.902 V_m \angle 18°$$

B. Modeling of Five-Phase Drive

The dynamic model of the induction motor is derived by using a two-phase motor in direct and quadrature (d-q) axes. For *d-q* model, different control schemes and experimentally obtained illustrations of performance for various MPIM (asymmetrical and symmetrical six-phase, and five-phase machines) are presented in [26]. Generalized *d–q* model of multi-phase machine with higher number of phases with commonly used simulation packages are reported in [27]. While modeling the 5-phase motor, the following assumptions are essential. The machine air gap is uniform, eddy current, friction and windage losses, and saturation are neglected, motor stator and rotor windings are sinusoidally distributed, windings are identical within each multi-phase set and there is no electrical interconnection between two multi-phase winding sets. The equivalence between the *3*-phase to *2*-phase machine model is derived from simple observation, and this approach is suitable for extending it to model a *n*-phase machine ($n>3$) by means of a *2*-phase machine. In *n*-phase induction machine, the spatial displacement between any two consecutive stator phases is $\alpha=2\pi/5$. The phase number *n* can be either odd or even. The machine model in original form is transformed using decoupling (Clarke's) transformation matrix [6]. In decoupling transformation matrix for an arbitrary phase number *n* can be given in power invariant form as shown in (6), where $\alpha=2\pi/n$. The first two rows of the matrix define variables that will lead to fundamental flux and torque production (d_1–q_1 components; stator to rotor coupling appears only in the equations for d_1–q_1 components).

Equations for pairs of d_2–q_2 components are completely decoupled from all the other components. These components do not contribute to torque production when sinusoidal distribution of the flux around the air-gap is assumed. A zero-sequence component does not exist in any star-connected multi-phase system. As stator to rotor coupling takes place only in d_1–q_1 equations, rotational transformation is applied only to these two pairs of equations. Assuming that the machine equations are transformed into an arbitrary frame of reference rotating at angular speed ω_e, the model of a *n*-phase induction machine with sinusoidal winding distribution is given by (6)-(22), which are identical to three-phase machines.

$$\begin{bmatrix} V_{d_1} \\ V_{q_1} \\ V_{d_2} \\ V_{q_2} \\ V_0 \end{bmatrix} = \sqrt{\frac{2}{5}} \begin{bmatrix} 1 & \cos\alpha & \cos 2\alpha & \cos 3\alpha & \cos 4\alpha \\ 0 & \sin\alpha & \sin 2\alpha & \sin 3\alpha & \sin 4\alpha \\ 1 & \cos 2\alpha & \cos 4\alpha & \cos\alpha & \cos 3\alpha \\ 0 & \sin 2\alpha & \sin 4\alpha & \sin\alpha & \sin 3\alpha \\ \sqrt{\frac{1}{2}} & \sqrt{\frac{1}{2}} & \sqrt{\frac{1}{2}} & \sqrt{\frac{1}{2}} & \sqrt{\frac{1}{2}} \end{bmatrix} \begin{bmatrix} V_a \\ V_b \\ V_c \\ V_d \\ V_e \end{bmatrix} \tag{6}$$

Stator circuit equations:

$$v_{ds} = R_s i_{ds} + \frac{d}{dt}\psi_{ds} - \omega_e \psi_{qs} \tag{7}$$

$$v_{qs} = R_s i_{qs} + \frac{d}{dt}\psi_{qs} + \omega_e \psi_{ds} \tag{8}$$

Rotor circuit equations:

$$v_{dr} = R_r i_{dr} + \frac{d}{dt}\psi_{dr} - (\omega_e - \omega_r)\psi_{qr} \tag{9}$$

$$v_{qr} = R_r i_{qr} + \frac{d}{dt}\psi_{qr} + (\omega_e - \omega_r)\psi_{dr} \tag{10}$$

Flux linkage expressions in terms of the currents are

$$\psi_{ds} = L_{ls} i_{ds} + L_m (i_{ds} + i_{dr}) \quad (11)$$

$$\psi_{dr} = L_{lr} i_{dr} + L_m (i_{ds} + i_{dr}) \quad (12)$$

$$\psi_{qs} = L_{ls} i_{ds} + L_m (i_{qs} + i_{qr}) \quad (13)$$

$$\psi_{qr} = L_{lr} i_{dr} + L_m (i_{qs} + i_{qr}) \quad (14)$$

$$\psi_{dm} = L_m (i_{ds} + i_{dr}) \quad (15)$$

$$\psi_{qm} = L_m (i_{qs} + i_{qr}) \quad (16)$$

$$i_{ds} = \frac{\psi_{ds}(L_{lr} + L_m) - L_m \psi_{dr}}{(L_{ls} L_{lr} + L_{ls} L_m + L_{lr} L_m)} \quad (17)$$

$$i_{qs} = \frac{\psi_{qs}(L_{lr} + L_m) - L_m \psi_{qr}}{(L_{ls} L_{lr} + L_{ls} L_m + L_{lr} L_m)} \quad (18)$$

$$i_{dr} = \frac{\psi_{dr}(L_{ls} + L_m) - L_m \psi_{ds}}{(L_{ls} L_{lr} + L_{ls} L_m + L_{lr} L_m)} \quad (19)$$

$$i_{qr} = \frac{\psi_{qr}(L_{ls} + L_m) - L_m \psi_{qs}}{(L_{ls} L_{lr} + L_{ls} L_m + L_{lr} L_m)} \quad (20)$$

where symbols R and L stand for resistance and inductance. While indices s and r identify the stator and rotor and index l stands for leakage inductances. v, i, Ψ, L_m, L_s, and L_r denote voltage, current, flux linkage, magnetizing inductance, stator leakage inductance and rotor leakage inductance respectively. The torque and speed equation is given with

$$T_e = pL_m (i_{qs} i_{dr} - i_{ds} i_{qr}) \quad (21)$$

$$\omega_r = \int \frac{p}{2J} (T_e - T_L)\, dt \quad (22)$$

C. SVPWM Technique

A detailed analyzes of SVPWM technique of five-phase VSI is reported in [25]. It is seen that the maximum voltage and minimum THD is observed in the large space vectors. In the large space vectors outer-most decagon in d_1 –q_1 plane is shown in Fig. 2. The input reference voltage vector is synthesised from two active vectors and zero space vectors respectively. The switching times are calculated by using the reference space vector $V_{ref,}$ magnitude of the larger plane and exact sector *(sec)* numbers of the different space vectors. The switching time sequence of active and zero space voltage vectors are derived from (23) & (24):

$$t_{al} = \frac{|\bar{V}_{ref}| \sin(\sec \pi/5 - \theta)}{|\bar{V}_l| \sin \pi/5} t_s$$
$$t_{bl} = \frac{|\bar{V}_{ref}| \sin(\theta - (\sec - 1)\pi/5)}{|\bar{V}_l| \sin \pi/5} t_s \quad (23)$$

$$t_0 = 0.5(t_s - t_{al} - t_{bl}) \quad (24)$$

where t_s =1/f_s; t_s- Sampling time; f_s-Sampling frequency equal to carrier frequency.

Fig. 3 shows the phasor diagram for large space vectors of five-phase VSI. It is seen that t_{al} and t_{bl} correspond to times of application of active large space vectors, where each sector starts with V_{al} and ends with V_{bl} respectively. In sector 1, t_{al} is the time of application of the voltage space vector V_{25}, while t_{bl} is the time of application of the voltage space vector V_{24}. t_0 and t_{31} are the time of application of zero voltage vectors of V_0 and V_{31}. For odd sectors, sequence of the switching period is *(t_0 t_{bl} t_{al} t_{31} t_{al} t_{bl} t_0)*, while in even sectors it is *(t_0 t_{al} t_{bl} t_{31} t_{bl} t_{al} t_0)*. The maximum possible fundamental peak voltage of large space vector is

$$V_{max} = |V_l| \cos(\pi/10) V_{dc} = 0.6155 V_{dc}$$

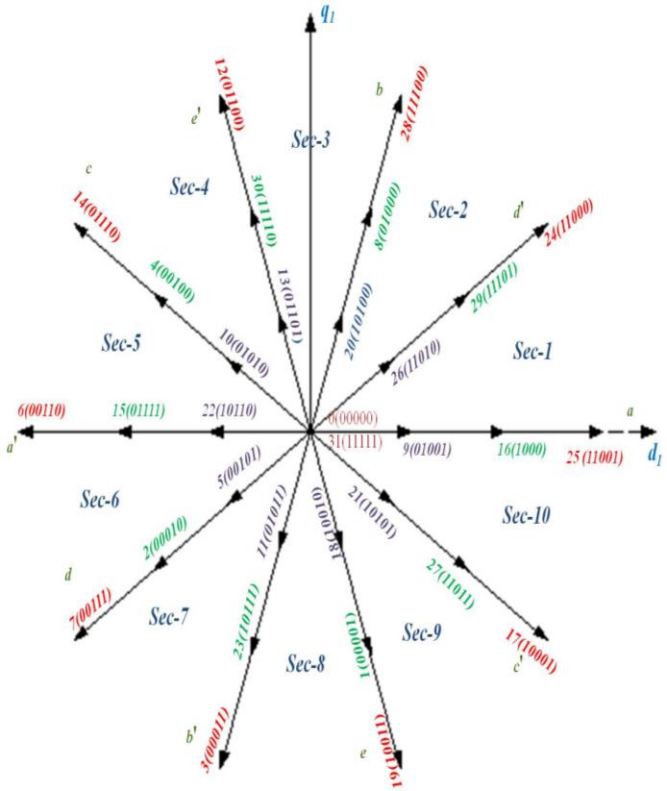

Fig. 2 Voltage space vector for 5-phase VSI

The switching pattern and space vector disposition sector 1 is shown in Fig. 4. It is seen that in one switching period it has two switching cycles. The first half of the switching cycle is zero space vector, two active large space vectors and the

second zero space vector. The second half of the switching cycle is mirror image of the first cycle.

The IFOC of 5-phase induction motor drive with experimental results are discussed elaborately in the following sections.

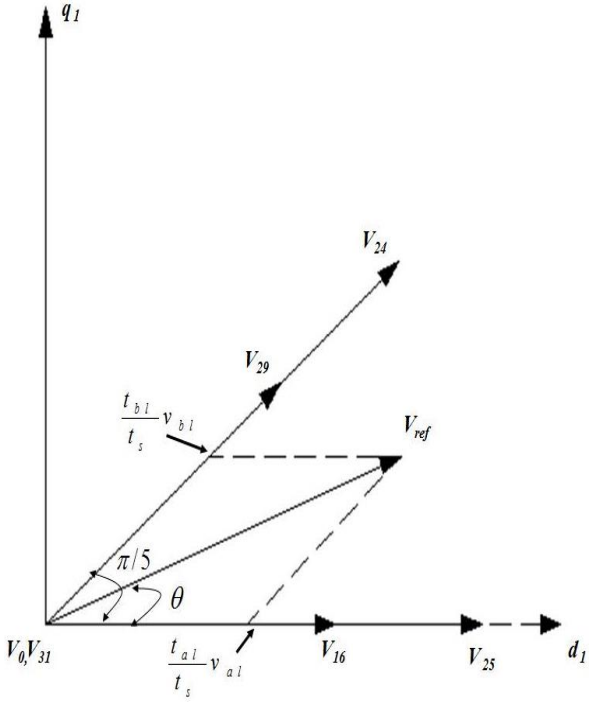

Fig. 3 Phasor diagram for large space vectors (sector 1)

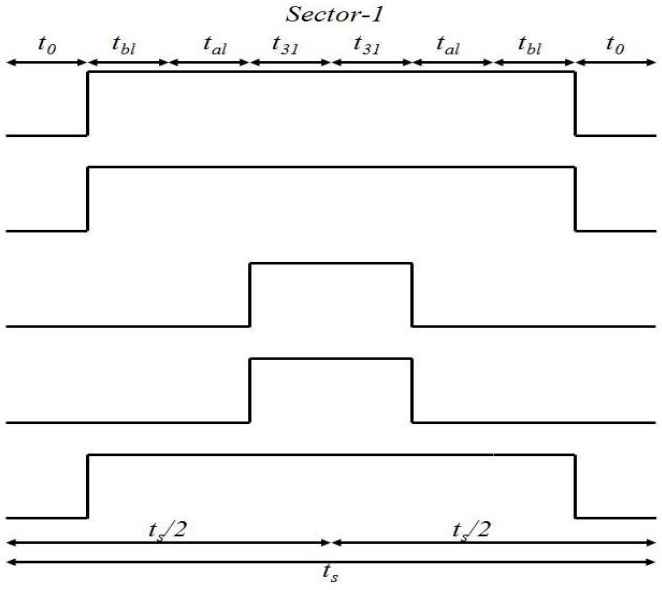

Fig. 4 Switching time sequence of large space vectors sector-1

III. Indirect Field Oriented Control of 5-Phase Induction Motor Drive

The schematic of indirect field oriented control (IFOC) of 5-Phase Inverter fed Induction Motor Drive is shown in Fig. 5. The IFOC of the 5-phase drive is of the same structure as the three phase drive [18]. The only difference is that the co-ordinate transformation now generates 5-phase current references instead of three. It is seen that the torque command is generated as a function of the speed error signal, generally processed through a PI controller. The commanded torque and flux producing components are processed through the different blocks. The 5-phase reference currents are compared with the actual current in the hysteresis band current controller and the controller takes the necessary action to produce PWM pulses to trigger the 5-phase inverter switches. The structure of the speed control loop is shown in Fig. 6. The transfer function of the speed controller is

$$G_{PI}(s)=K_p(1+\frac{1}{sT_i})=K_p+K_i\frac{1}{s} \quad (25)$$

$$1+G_{PI}(s)H(s)=0 \quad (26)$$

$$S^2+66.67k_pS+66.67K_i=0 \quad (27)$$

The coefficients in the above equation are equated with those in the following equation, which defines the desired closed loop dynamics in terms of the damping ratio ξ and natural frequency ω_0.

$$S^2+2\xi\omega_oS+\omega_o^2=0 \quad (28)$$

where damping ratio is 0.707, and frequency as 10 Hz, from that K_p and K_i values are found to be 1.3325 and 59.2156.

IV. Simulation Results

The inverter fed induction motor model is simulated to investigate the performance of the drive under varying loads. The parameters of the 1 hp induction motor is given in Table I is used for simulation. The large space vector technique is used to generate pulses for inverter as it is effective in terms of THD and fundamental voltage. The voltage, current, torque and speed are observed for different step change in torque conditions.

The closed loop response is studied for different speed and torque conditions. Fig. 7 shows the simulation results of 5-phase drive at step change in torque condition. It is seen that the controller tracks the reference speed and motor torque follows the load torque. Simulation is repeated for step change in speed condition and shown in Fig. 8. From the results obtained, it is seen that the controller tracks the reference speed and torque effectively.

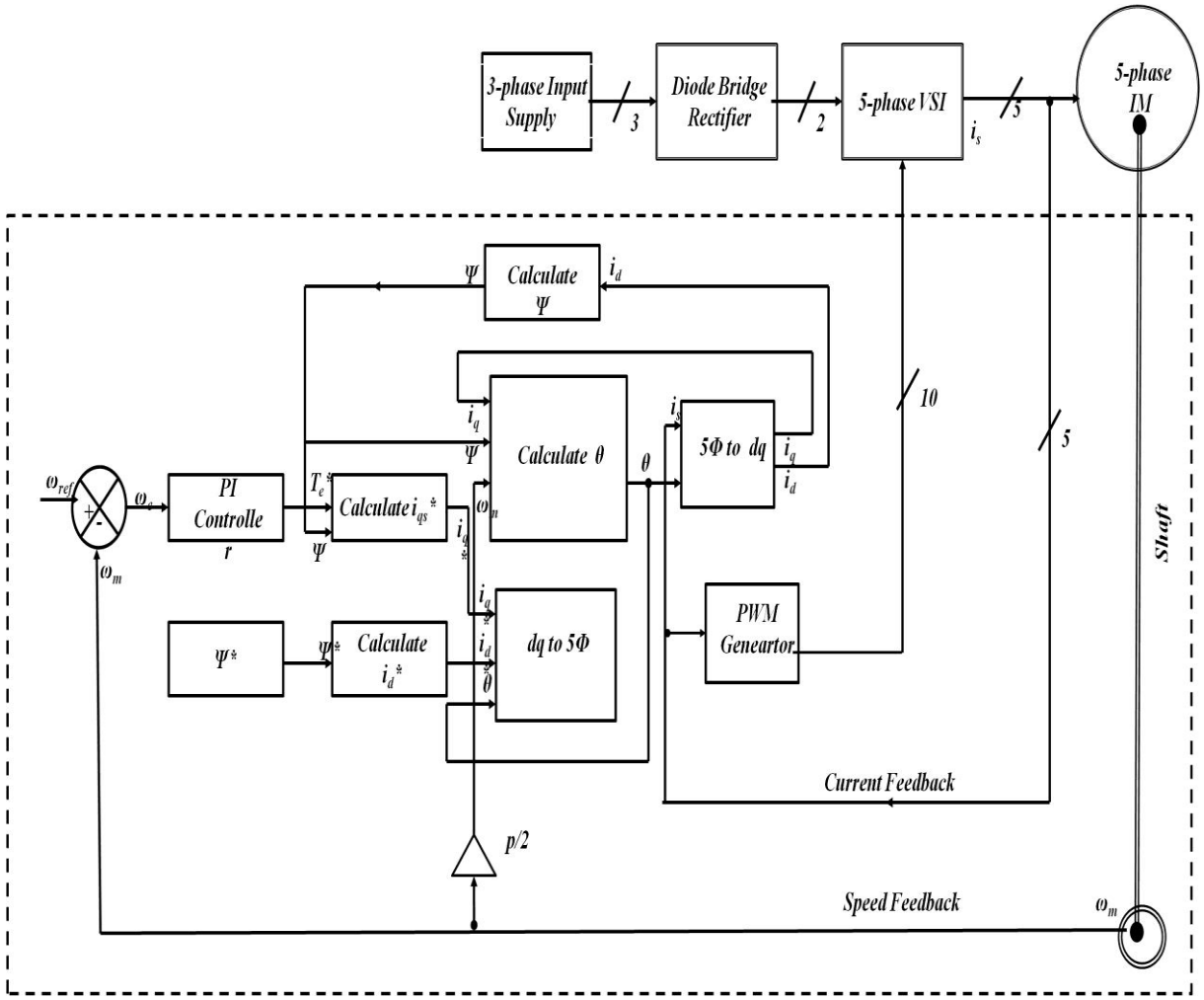

Fig. 5 Block Diagram of IFOC of 5-Phase Inverter fed Induction Motor Drive

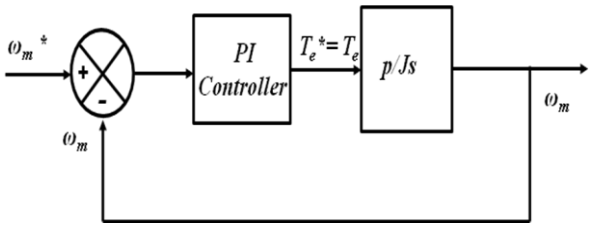

Fig. 6 Structure of the speed control loop

V. Experimental Setup

The schematic diagram of an experimental 5-phase induction motor drive is shown in Fig. 9. It consists of three phase auto-transformer (600V/6A), uncontrolled rectifier, 5-phase VSI and 5-phase induction motor with loading arrangement. The specifications of the hardware arrangement are presented in Table I. The PEC16DSM013 IPM (Intelligent power module) consists of five-phase VSI assembled with ten insulated gate bipolar transistors (IGBT) of rating 300V/15A. The proposed control algorithm is implemented in digital platform using the XC3SD1800A Spartan-3A FPGA processor. Its clock frequency is 20 MHz. The FPGA processor is interfaced to the system through the dedicated interface card. The control algorithm is written in VHDL coding in XILINX platform. The Spartan-3A FPGA generates ripple free PWM signals at a switching frequency of 10 kHz. The signals are fed to the inverter switches through the gate driver circuit. The inverter output is observed through the four channel Agilent oscilloscope and 6-channel YOKOGAWA WT1800 precision power analyzer as shown in Fig. 10.

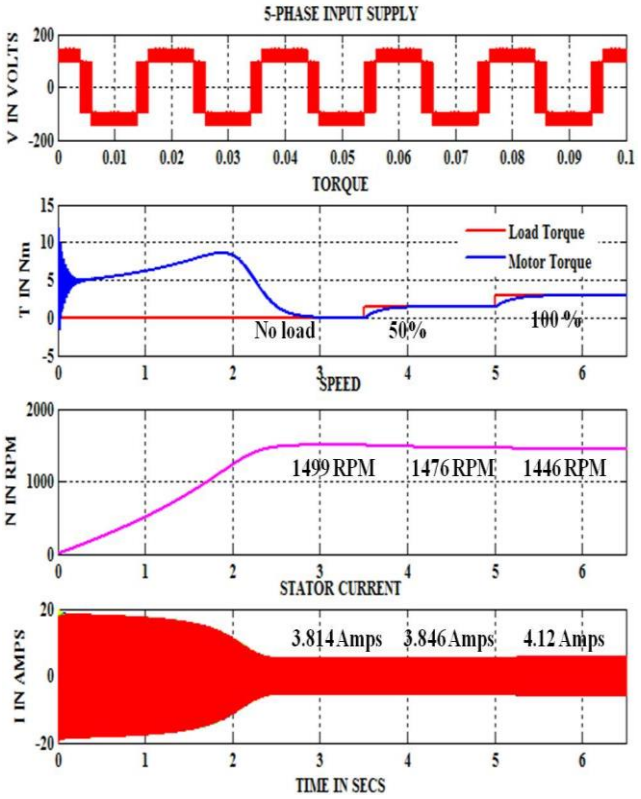

Fig. 7 Response of the drive at step change in torque condition

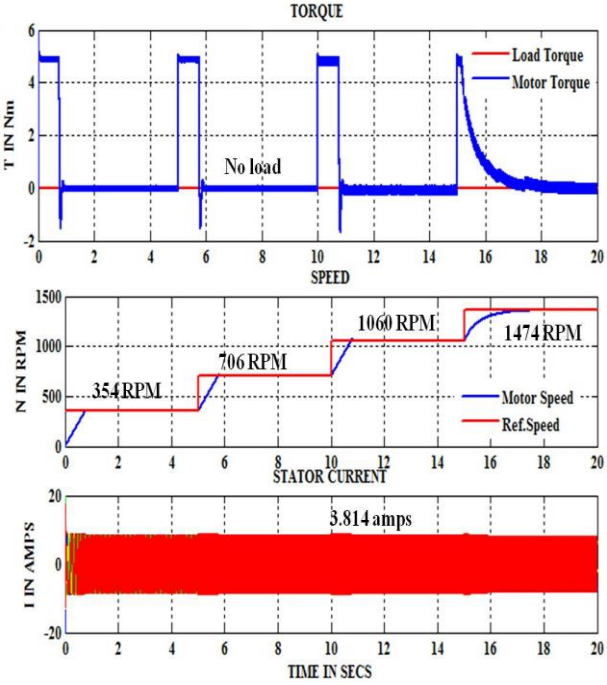

Fig. 8 Response of the drive for step change in speed condition

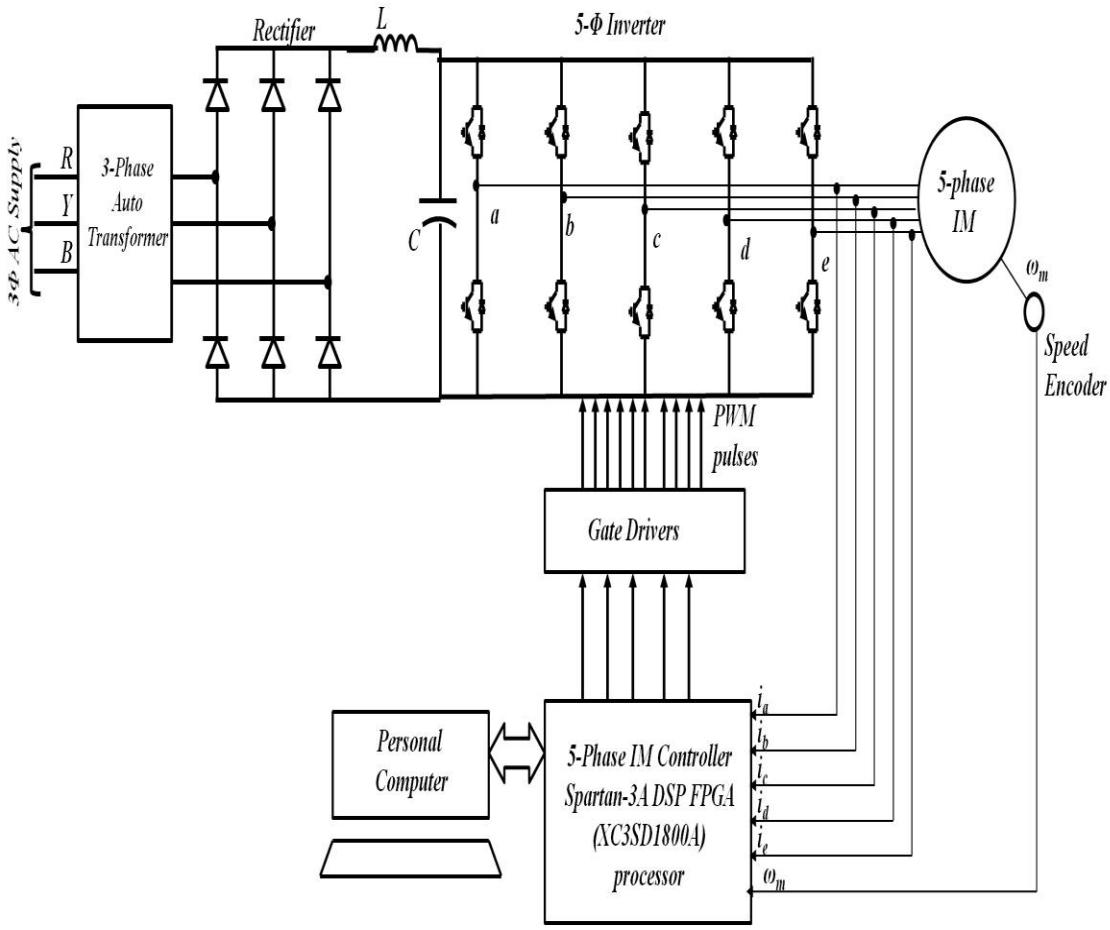

Fig. 9 Experimental Setup for 5-Phase Inverter fed Induction Motor Drive

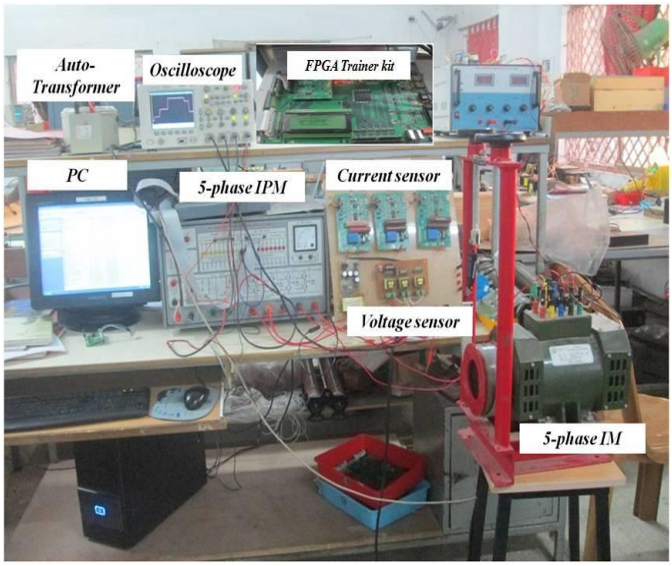

Fig. 10 Experimental Test-Rig

VI. Experimental Results

The experimental setup of the 5-phase induction motor is used to validate the simulation model of the 5-phase inverter fed induction motor drive. Figs. 11 (a)-(e) show experimental results at rated voltage of 104 V_{ph} and frequency of 50 Hz. Fig. 11 (a) shows the modulating signals for 5-phases using large space vector technique. The modulating signals are compared with high frequency carrier signals and produce a SVPWM pulses for upper switches is shown in Fig. 11 (b). The complimentary of the SVPWM pulses are used for lower switches. Fig. 11 (c) shows the dead time of 6μs to prevent the short circuit of the switches in the same leg. The line voltage and phase voltage of 198 volts and 104 volts are observed from Fig. 11 (d). The 5-phase load current is shown in Fig. 11 (e) with 72° phase displacement. Fig. 12 shows the step change in speed, the controller tracks the reference speed from low speed to rated speed condition. Fig. 13 shows the comparison of simulated and experimental results for different reference speed condition. From the results, it is observed that the experimental results closely match with the simulation findings. Thus the simulation model is validated and it can be used to predict for n number of phases.

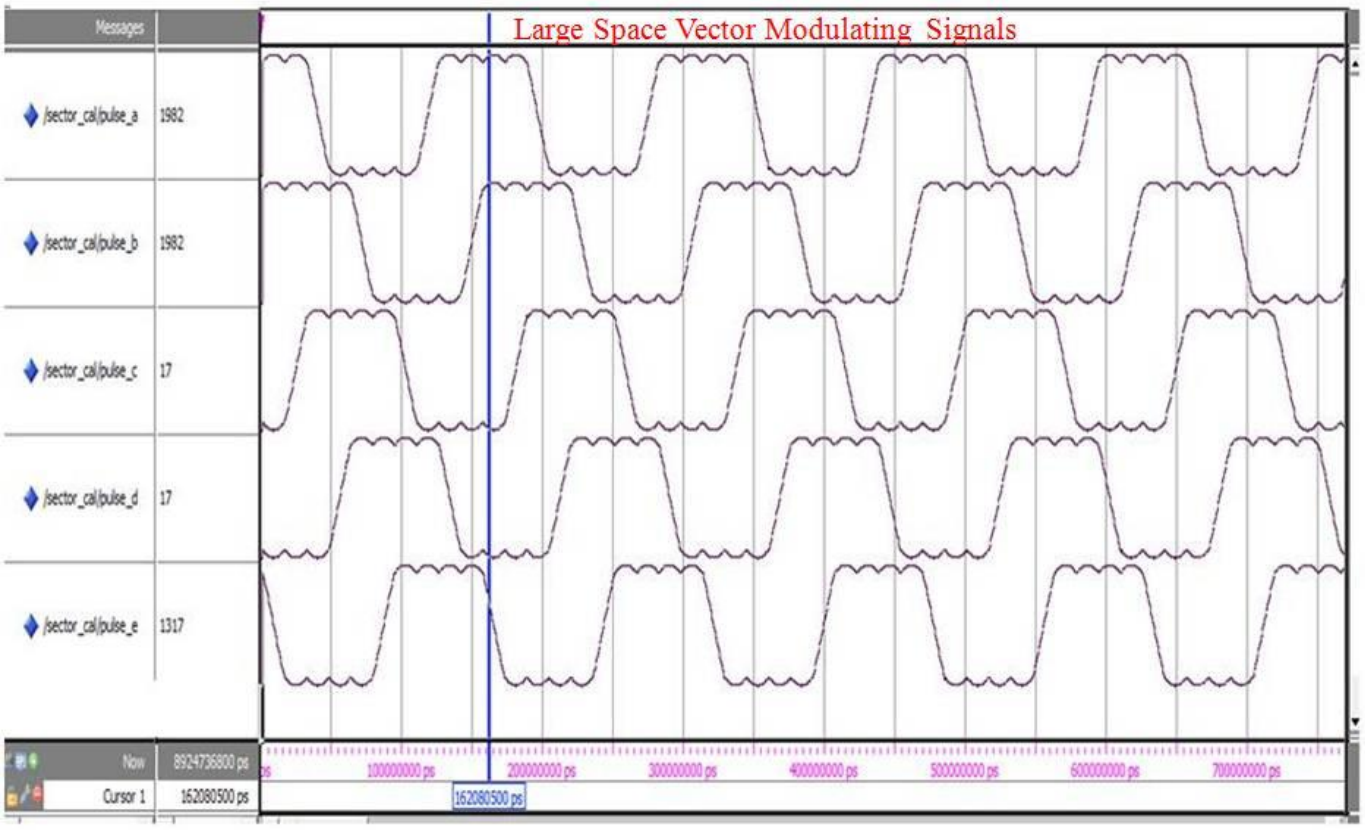

(a)

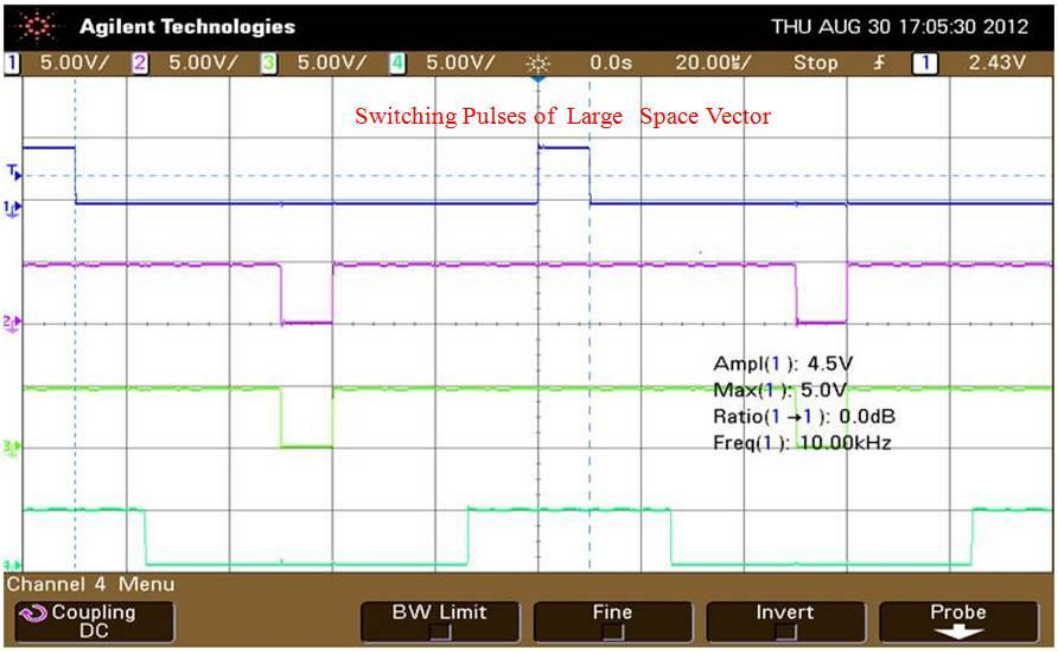

(b)

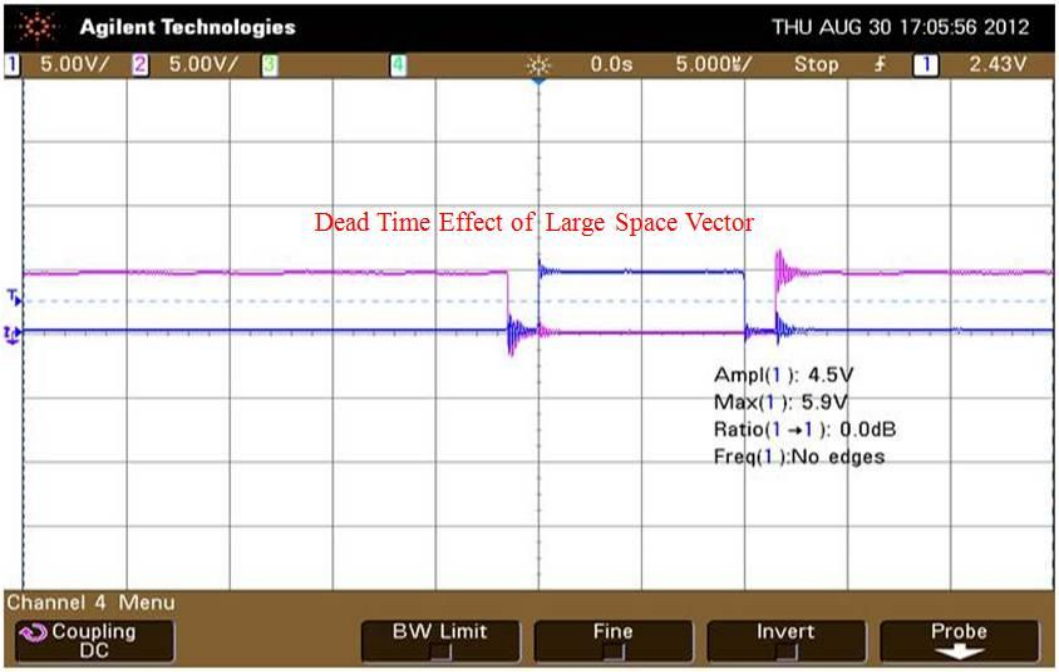

(c)

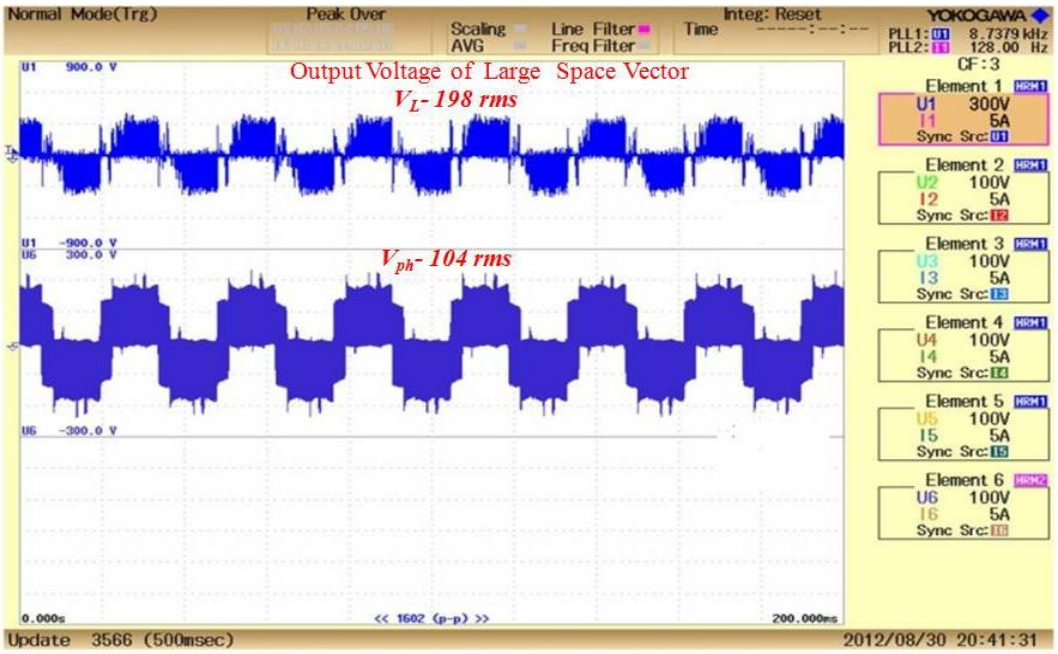

(d)

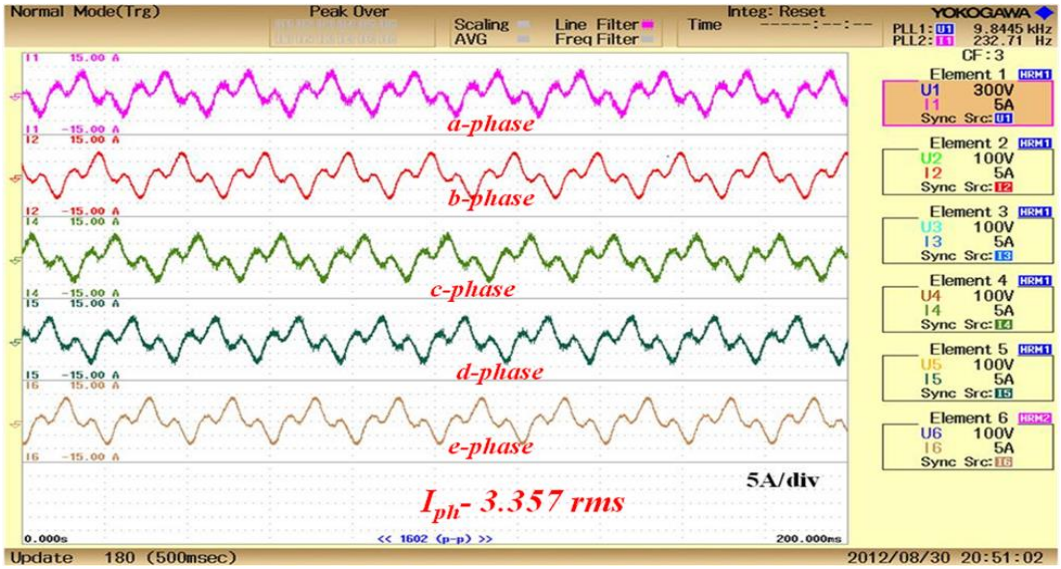

(e)

Fig. 11 Experimental results (a) Modulating signal (b) PWM pulses (c) Dead time effect (d) Line and phase voltage (e) Stator current

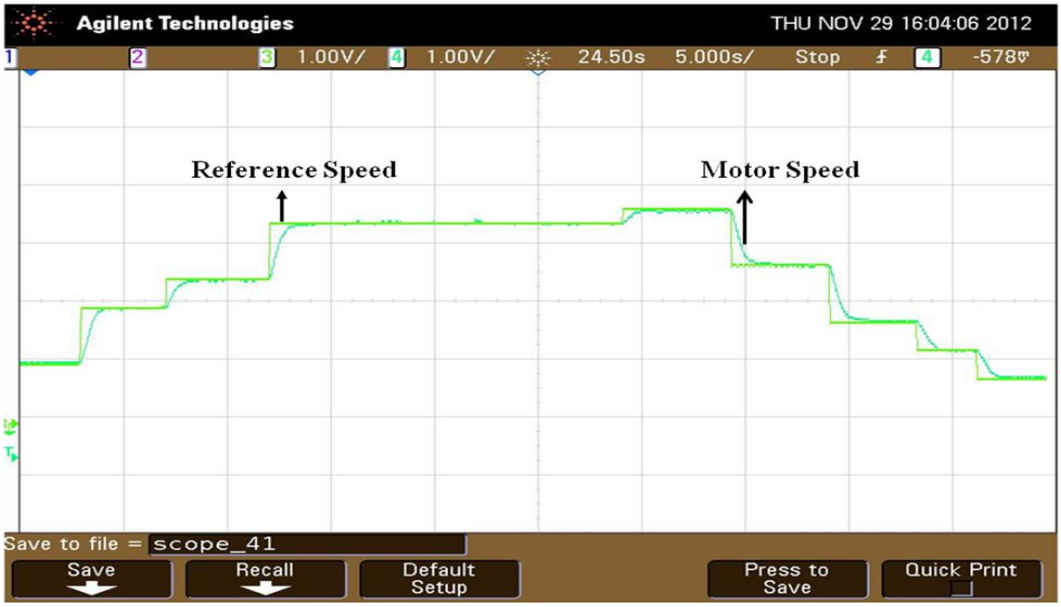

Fig. 12 Experimental result of step change in speed

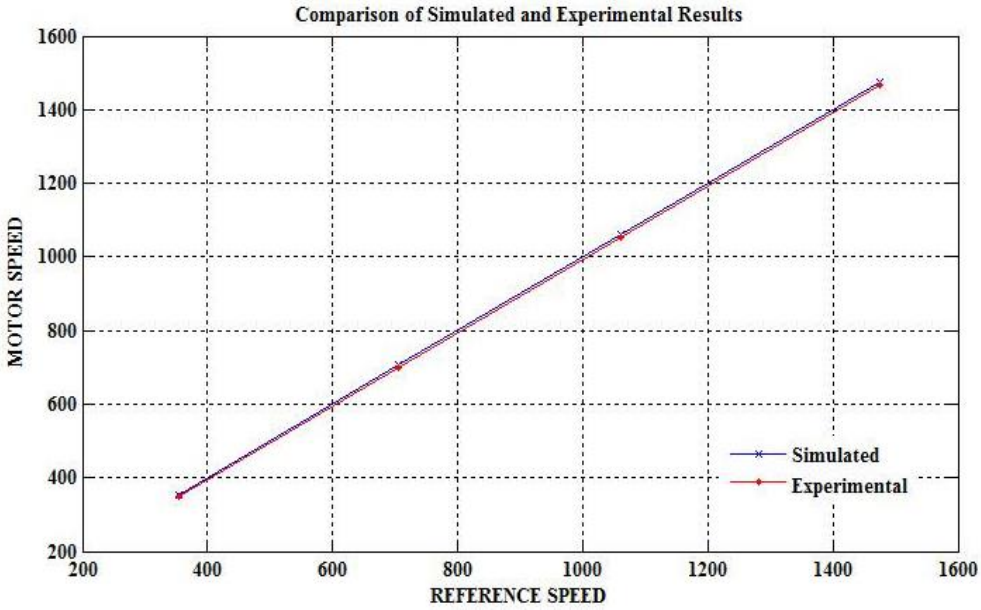

Fig. 13 Comparison of simulated and experimental results

TABLE I
PARAMETERS OF FIVE- PHASE INDUCTION MOTOR DRIVE

Parameters	Values
Power	1 hp
Phase	5-phase
Frequency	50 Hz
No. of poles	4
Stator resistance (R_s)	5 ohm
Rotor resistance (R_r)	2.8 ohm
Stator leakage inductance (L_{ls})	0.01759 H
Rotor leakage inductance (L_{lr})	0.01759 H
Mutual inductance (L_m)	0.12 H
Inertia (J)	0.01 kg.m^2
Friction (F)	0. 15N.m.s

VII. CONCLUSION

The simulation model of the 5-phase VSI fed induction motor drive is developed in MATLAB/Simulink environment. The SVPWM techniques are expressed in VHDL coding by using XILINX XC3SD1800A FPGA processor. The closed loop response of the drive is studied with an indirect field oriented controller. The output current, speed and torque are observed. From the simulation results it is found that the controller tracks the reference speed in the different operating range from no load to full load. The experimental result for 5-phase inverter fed 1 hp induction motor drive is obtained. The experimental results are compared with simulation findings and validate the model developed.

REFERENCES

[1] E. Levi, R. Bojoi, F. Profumo, H.A. Toliyat and S. Williamson, "Multiphase induction motor drives-A technology status review," *IET Elect. Power Appl.* vol. 1, no. 4, pp. 489-516, July 2007.

[2] E.E. Ward and H. Harer, "Preliminary investigation of an inverter fed five-phase induction motor", *Proc. IEE* 116 (6), 1969, pp. 980- 984.

[3] T.M. Jahns, "Improved reliability in solid-state AC drives by means of multiple independent phase-drive units", *IEEE Transactions on Industry Applications*, vol. IA-16, no. 3, may. -jun.1980, pp. 321-331.

[4] S. Williamson and A.C. Smith, "Pulsating torque and losses in multiphase induction machines", *IEEE Trans. Ind. Appl.*, vol. 39, no. 4, pp. 986-993, July/Aug. 2003.

[5] M. A. Abbas, R. Christen, and T. M. Jahns, "Six-phase voltage source inverter driven induction motor," *IEEE Trans. Ind. Applicat.*, vol. IA-20, no. 5, pp. 1251–1259, Sept./Oct. 1984.

[6] R. Lyra and T.A. Lipo, "Torque density improvement in a six-phase induction motor with third harmonic current injection", *IEEE Trans. Ind. Appl.* Vol. 38, no. 5, pp. 1351-1360, Sept./Oct. 2002.

[7] M. Apsley and Williamson, "Analysis of multi-phase inductions with winding faults", *Proc. IEEE IEMDC,* San Antonio, TX, pp.249-255, 2005.

[8] J.M. Apsley, S. Williamsons, A.C. Smith and M. Barnes, "Induction motor performance as a function of phase number", *Proc.Int. Electr. Eng.-Electr. Power Appl.*, vol. 153, no. 6, pp. 898-904, Nov. 2006.

[9] Boglietti, R. Bojoi, A. Cavagnino, and A. Tenconi, "Efficiency analysis of PWM inverter fed three-phase and dual three-phase induction machines," in *Conf. Rec. IEEE IAS Annu. Meeting*, Tampa, FL, 2006, pp. 434–440.

[10] D. Dujic, M. Jones, and E. Levi, "Analysis of output current ripple rms in multiphase drives using space vector approach", *IEEE Trans. On Power Elect.*, vol. 24, no. 8, pp. 1926-1938, Aug. 2009.

[11] A. Toliyat, T.A. Lipo and J.C. White, "Analysis of concentrated winding machine for adjustable speed drive applications-Part II: Motor design performance", *IEEE Tras. Energ Conv.*, vol. 6, no. 4, pp. 684-692, Dec. 1991.

[12] Y. Zhao and T. A. Lipo, "Modeling and control of a multi-phase induction machine with structural unbalance. Part I: Machine modeling and multi-dimensional current regulation," *IEEE Trans. Energy Convers.*, vol. 11, no. 3, pp. 570–577, Sep. 1996.

[13] Y. Zhao and T. A. Lipo, "Modeling and control of a multi-phase induction machine with structural unbalance. Part II: Field-oriented control and experimental verification," *IEEE Trans. Energy Convers.*, vol. 11, no. 3, pp. 578–584, Sep. 1996.

[14] E. A. Klingshirn, "High phase order induction motors-Part I-Description and theoretical considerations," *IEEE Trans. Power App.Syst.*, vol. PAS-102, no. 1, pp. 47–53, Jan. 1983.

[15] E. A. Klingshirn, "High phase order induction motors-Part II-Experimental results," *IEEE Trans. Power App. Syst.*, vol. PAS-102, no. 1, pp. 54–59, Jan. 1983.

[16] Leonhard, W. 1995. ''Controlled AC Drives, A Successful Transfer from Ideas to Industrial Practice''. CETTI 95. Brazil, pp. 1-12.

[17] MacDonald, M.L. and P.C. Sen. 1979. ''Control Loop Study of Induction Motor Drive Using D-Q Model'' *IEEE Transaction on Industrial Electronics and Control Instrumentation*, 26(4):237-241.

[18] B.J. Bose, *Power Electronics and Variable Frequency Drives,* IEEE press,1996.

[19] R. Ortega, D. Taoutaou, "Indirect field-oriented speed regulation for induction motors is globally stable," *IEEE Trans.* on *Industrial Electronics,* 43(2), 340-341,1996.

[20] L. U. Gokdere, M.A. Simaan, C.W. Brice, "Global asymptotic stability of indirect field-oriented speed control of induction motors," Automatica, vol.34, no.1, pp.133-135, Jan.1998.

[21] R. Marino, S. Peresada, P. Tomei, "Output feedback control of current-fed induction motors with unknown rotor resistance," *IEEE Trans.* on *Control System Technology,* 4(4), 336-347, 1996.

[22] F. Blaschke, 'The principle of field orientation as applied to the new transvector closed-loop control system for rotating-field machines," *Siemens Rev*., vol. 34, pp. 217–220, 1972.

[23] Atif Iqbal, Sk. Moin Ahmed and Haitham Abu-Rub "A Modeling, Simulation and Implementation of a Five-Phase Induction Motor Drive System" 978-1-4244-7781-4/10, 2010.

[24] H. Xu, H. A. Toliyat, and L. J. Petersen, "Five-phase induction motor drives with DSP-based control system," in *Proc. IEEE IEMDC*, Cambridge, MA, 2001, pp. 304–309.

[25] G. Renukadevi and K. Rajambal, "Field Programmable Gate Array Implementation of Space-Vector Pulse-Width Modulation Technique for Five-Phase Voltage Source Inverter," *IET Power Electronics*, ISSN 1755-4535, pp.376-389.

[26] E. Levi, "Multiphase Electric Machines for Variable Speed Applications," *IEEE Transactions on Industrial Electronics*, vol. 55, no. 5, pp. 1893-1909, MAY 2008.

[27] G. Renukadevi and K. Rajambal, "Generalised d-q model of n-phase induction motor drive," *International journal of electrical engineering, World Academy of Science, Engineering and Technology*, Vol:6 No:9, 2012, pp.1216-1225.

G. Renuka Devi received her Undergraduate Degree in Electrical Engineering from The Institution of Engineers, India in 2006 and M.Tech in Electrical Drives and Control from Pondicherry Engineering College in 2009, Ph.D in Multi-Phase Drive Systems from Pondicherry University in 2016. She is working as Associate professor in the Department of Electrical and Electronics Engineering in Manakula Vinayagar Institute of Technology, Puducherry. Her field of interest is power electronics, Drives and control, AI techniques and control systems. She has published papers in international journals and conferences in the field of Electrical Drives and Power Electronics.